Proceedings of the Indian National Science Academy (2023) 89:924–940
https://doi.org/10.1007/s43538-023-00209-2

RESEARCH PAPER

Real-time weather data analysis by the solar fuzzy logic-based MPPT controller

Harsh Bhati[1] · **Lata Gidwani**[1]

Received: 15 June 2023 / Accepted: 1 September 2023 / Published online: 18 September 2023

Abstract

The performance of a solar (PV) system with a boost converter using maximum power point tracking (MPPT) control algorithms is studied in this article. The primary goals of the latest renewable energy systems are to harvest the maximum amount of power possible from high-penetration renewable energy sources and to step up the low voltage to the required voltage level with low-power semiconductor switches. Mostly in the current study period, MPPT control technology and power converter are available. This study uses real-time data from the PV system in the area of 25.1383°N, 75.8076°E in India to analyze the boost converter or in this location, there is a change in the maximum power generated in a day due to changes in weather conditions and how much longer we can find the maximum power output due to the fluctuations. The boost converter has less switching loss and voltage stress. The FL-MPPT controller is taken into account while evaluating the effectiveness of the MPPT approach in a PV system, and the findings demonstrate that it provides the best and most steady output.

Keywords MPPT · PV system · Renewable energy source · Boost converter · Fuzzy logic controller

Introduction

National economic growth relies on energy. It's essential to everyday life and a nation's socioeconomic progress and well-being. A country with high energy consumption will have more household, agricultural, transportation, and industrial activities, raising living standards. Thus, per capita, energy consumption indicates prosperity and quality of life. But the growing energy supply-demand imbalance is a worry. Science and academia have considered several solutions to this issue, with solar energy being the most promising. Solar energy is eco-friendly and has several advantages. Sustainability, renewable energy, and decreased fossil fuel dependence are its advantages. Solar energy saves money, creates employment, and boosts the economy. Its scattered generation and off-grid options make it beneficial. Research and development enhance solar energy's efficiency and cost. Solar energy integration requires supportive legislation, infrastructure spending, government, industry, and community engagement. Since fossil fuel consumption in the electricity sector has developed rapidly, concerns about its environmental effects have intensified. As is known, current research focuses on renewable green energy sources to identify clean and affordable energy sources, extract the most energy from available sources, and convert low-rated energy sources into the required energy level using the latest power semiconductor techniques (Kumar et al. 2018). Due to its broad availability, clean, quiet operation, and absence of pollutants, PV has garnered attention, according to the research. Solar electricity produces less voltage. Various converter types and Maximum PowerPoint tracking approaches are needed to improve this low-voltage profile. The authors reviewed MPPT-based PV system literature from 2010 to 2017. The writers also stressed maximizing renewable PV electricity. A literature study improved power electronic converter voltage transfer conversion gain. The converter circuit's voltage conversion gain depends on the power semiconductors and reactive power components employed. The operational duty cycle time determines converter topology structure, gain levels, efficiency, and switching stress. When the ideal connection is known, hill climb search (HCS) or perturb and observe (P&O) MPPT is utilized. The P&O technique tracks the optimum point

✉ Harsh Bhati
harsh.20mtps807@rtu.ac.in

Lata Gidwani
lgidwani@rtu.ac.in

[1] Department of Electrical Engineering, Rajasthan Technical University, Kota, India

by continually modifying the maximizing variable and measuring the extracted power. The perturbation quantity and direction are determined repeatedly until the technique achieves the ideal point based on power variation and perturbation operation. The control system inputs dc-link components like current and voltage and outputs a duty cycle from the converter switch. This reduces system complexity and improves dependability. The P&O algorithm's only downside is its fast convergence when light changes. The P&O system output rotates around the MPP during irradiance fluctuations until the input system stabilizes. The soft computing-based maximum power point tracking method works as a fuzzy logic controller (FLC). FLC can compensate for P&O controller flaws (Eltamaly et al. 2018). Soft computing techniques have faster convergence and response times during PV system irradiance and temperature fluctuations. The FLC-based MPPT controller requires just system characteristics, making installation easier than P&O. Fuzzy logic controllers promote stability in non-linear systems. This research analyzes MATLAB/Simulink to evaluate the efficiency of a PV system with a boost converter using real-time solar irradiation data for 25.1383°N, 75.8076°E. The new system's efficiency is assessed using continuous irradiation data of 800 W/m^2 at 25 °C under conventional test conditions and time-varying data from February 10, 2023 to February 25, 2023. The MATLAB/Simulink results and output power throughout the selected periods are compared. PV systems are depicted in Fig. 1. The FLC-based maximum power point tracking controller determines the maximum power extraction duty cycle.

The paper is structured as follows: Part 2 discusses the modelling of the Solar PV system that is employed in the proposed model. The modelling of the boost converter and its parameters is discussed in Modeling of PV module section, along with how they were employed for the suggested design. In Boost Converter (DC-DC) section, we will discuss both the structure and operation of the FLC-based MPPT approach. In Maximum power point tracker (MPPT) section, we will demonstrate how integrating MATLAB/Simulink with the suggested system would provide the desired results. The conclusions drawn from the evaluation of the proposed system are presented in Fuzzy logic controller section.

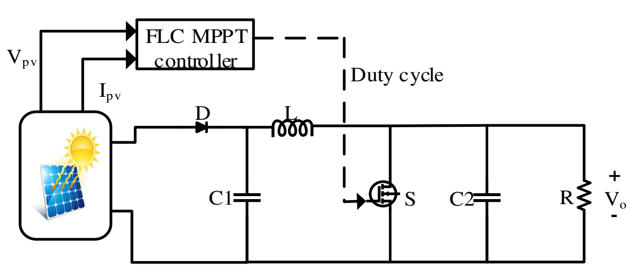

Fig. 1 Block diagram of proposed system

Solar photovoltaic system (SPV)

A collection of photovoltaic cells is a solar PV array, and it's what turns the sun's rays into electricity. A single PV cell cannot deliver sufficient electricity for typical day-to-day activities. When there is a desire for high voltage, the required power may be attained by connecting several single PV cells in series, however, when there is a demand for high current, the cells must be linked in parallel (Wang et al. 2019). The term "module" refers to the arrangement of PV cells in either a serial or parallel fashion. The standard commercial module has either 36 or 72 individual cells. Variations in the array's internal series resistance are the reason for the efficiency of the solar device. There will be no change in efficiency brought on by variations in the shunt resistance. The schematic representation of the electrical equivalent circuit of a Solar PV system may be seen in the Figure. A photocurrent source (I_{ph}), a series resistor (R_s), a parallel resistor (R_{sh}), and a diode (D) are all components of the corresponding circuit. In this, a comprehensive discussion is held over the mathematical modeling of the SPV system. When Kirchhoff's current law is used, the following equation for the current that flows through a Photovoltaic (PV) systems cell is obtained:

$$I_{Ph} = I_{PV} + I_D + I_{Sh}, \tag{1}$$

$$I_{PV} = I_{Ph} - I_D - I_{Sh}, \tag{2}$$

where I_{PV} is the output of the SPV cell, Iph is the current passing through the photons, I_D is the current flowing through the diode, and I_{sh} is the current flowing through the R_{sh} (see Fig. 2).

Modeling of PV module

The mathematical model of the PV module is presented here in Eq. (3). With this model, the only thing that has to be done is to compute the parameter that determines how well the curve fits, which can be gotten directly out of the Eq. (3). The

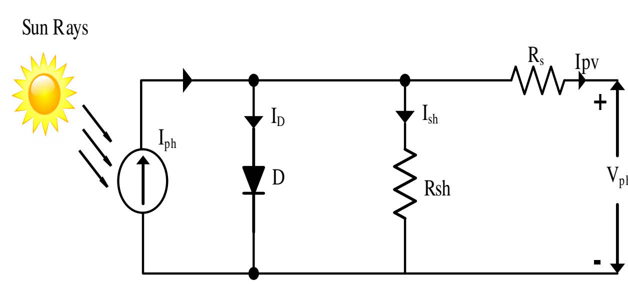

Fig. 2 Electrical equivalent circuit of an SPV cell

electrical data of the PV module is used to derive the other characteristics that are used.

$$I(V) = \frac{Ix}{1 - e^{\left(\frac{-1}{b}\right)}}\left[1 - e^{\left(\frac{V}{bV_X} - \frac{1}{b}\right)}\right], \tag{3}$$

where Vx and Ix are the open circuit voltage and short circuit current, respectively, with dynamic values for solar irradiation and temperature, which are determined by Eqs. (4) and (5); b is the characteristic constant, which has no units and is the only quantity that has to be computed.

$$\begin{aligned} Vx = s\frac{Ei}{EiN}TCv(T - Tn) + sV\mathrm{max} \\ - S(V\mathrm{max} - V\mathrm{min})e^{\left(\frac{Ei}{EiN}In\left(\frac{V_{\mathrm{max}} - V_{OC}}{V_{\mathrm{max}} - V_{\mathrm{min}}}\right)\right)}, \end{aligned} \tag{4}$$

$$I_x = p\frac{Ei}{EiN}\left[I_{sc} + TCi(T - Tn)\right], \tag{5}$$

where, S = Number of PV modules connected in series. p = Number of PV modules connected in parallel. Ei = Effective irradiation of the PV module. EiN = Constant Irradiation. T = Temperature of the PV module. Tn = Constant Temperature. TCv = Temperature coefficient of voltage. TCi = Temperature Coefficient of current. Voc = Open circuit voltage. Isc = Short circuit current. Vmax = Maximum voltage for irradiations (this value is 103% of Voc). Vmin = Minimum voltage for irradiations (this value is 85% of Voc).

The approximate solution of Eq. (6) may be performed by knowing that the value of b lies between 0.01 and 0.18.

$$1 - e^{\left(\frac{-1}{b}\right)} \approx 1. \tag{6}$$

Boost converter (DC–DC)

The use of hardware circuits called DC-DC converters allows for the efficient transfer of power between various circuits operating at varying DC voltage levels. To maximize the power output of Photovoltaic, several DC–DC converters, also known as boost converters, are used. The most widely used converters in DC–DC converters are boost converters, which raise the voltage from their contribution to output. A regulated switch (S), a diode (D), an energy storage inductor (L), and a capacitor make up the boost converter. The load connects the filter capacitor (C) at the output side as indicated in Fig. 3. The boost converter's output voltage (V_O) is then assessed under the steady-state operation represented by Eq. (9) (Kumar et al. 2017).

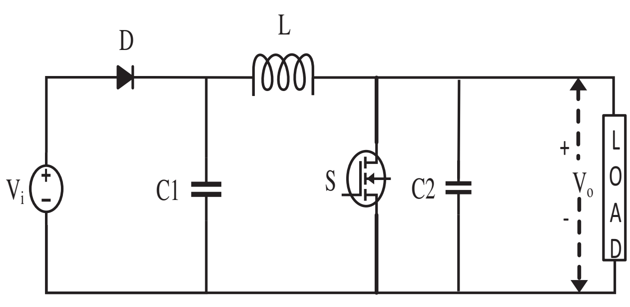

Fig. 3 Structure of Boost converter (DC-DC)

$$D = 1 - \frac{\left(V_{i_{\min}} * n\right)}{V_o}, \tag{7}$$

$$\frac{V_o}{V_i} = \frac{1}{(1 - D)}, \tag{8}$$

$$V_o = \frac{V_i}{(1 - D)}, \tag{9}$$

where V_i and D stand for input voltage and duty cycle, n stand for efficiency respectively. Inductor selection the higher the inductor value the higher is maximum output current because of reduced ripple current. The Eq. (10) is a good estimation for the right inductor.

$$L = \frac{V_i * \left(V_o - V_i\right)}{\Delta I_L * f_s * V_o}, \tag{10}$$

Vi = Input voltage, Vo = Output voltage, fs = minimum switching frequency of the converter, ΔI_L = inductor ripple current.

A good estimation for the inductor ripple current is 20–40% of the output current.

$$\Delta I_L = (0.20\,\text{to}\,0.40) * I_{o_{\max}} * \frac{V_o}{V_i}, \tag{11}$$

ΔI_L = Inductor ripple current, I_{omax} = maximum output current.

Due to the switching power supply's peak current need, an input side capacitor must have a minimum value in order to stabilize the input voltage. Due to the switching power supply's peak current need, this minimal number is required to stabilize the input voltage. Otherwise, the capacitor may lose a significant amount of its capacitance owing to temperature or DC bias. Output side capacitor value for the desired output voltage ripple can be determine by the Eq. (12).

$$C_{out} = \frac{I_{o_{\max}} * D}{f_s * \Delta V_o}, \tag{12}$$

C_{out} = minimum output capacitance, Io_{max} = maximum output current, D = duty cycle calculate by Eq. (8), f_S = switching frequency of the converter, ΔV_o = Desired output voltage ripple

Maximum power point tracker (MPPT)

A pure and limitless source of energy is photovoltaic energy. Installing PV, however, comes at a considerable initial expense. The output power must thus be increased while keeping the number of Photovoltaic module constant (Kumar et al. 2017). Solar irradiation and temperature both affect the PV array's output power. As a result, monitoring the maximum power point of the PV array stated is required to maximize the efficiency of the renewable energy system. The PV array has a particular operating point where it can supply the load with the most significant amount of power (Ibrahim et al. 2021). The maximal power point is located here (MPP). This point's location varies nonlinearly with both cell temperature and solar irradiation. Thus, the Photovoltaic system must have a maximum power point tracking (MPPT) controller to run the PV module at its MPP. The control parameter of an MPPT controller is the duty cycle. Under solar irradiance and temperature, the MPPT controller adjusts the duty cycle to its ideal value. The power circuit and the controller are the two components of the MPPT circuit (Pillai et al. 2018) (see Fig. 4).

Fuzzy logic controller

Fuzzy logic is a method for producing definite, acceptable outcomes from imperfect inputs. FL produces judgments that lie between the values of YES and NO and are comparable to human judgments. FL is capable of handling nonlinearities and does not require exact inputs. The input variables for the fuzzy controller are the P–V slope and the changes in slope. The main benefit of employing this method is that it can easily measure the operating point and the Maximum Power Point, making the duty cycle increase or decrease possible. Changes in slope can also be used to determine the operating point's movement direction in order to prevent variations. Fuzzy rules are developed using fuzzy input variables. There are four crucial steps in the FL system as shown in Fig. 5. Error and change in error (E and △E) input is for the fuzzy system to take into account. The duty ratio of the controller is provided by the FL system's output. Equation (13), and (14) provide E and △E (Saravanan and Babu 2016).

$$E(n) = \frac{P(n) - P(n-1)}{V(n) - V(n-1)}, \tag{13}$$

$$\Delta E(n) = E(n) - E(n-1). \tag{14}$$

In this case, n stands for the iteration number, E stands for error, △ E stands for change in error, P stands for power, and V stands for voltage. The duty cycle of the system, which is provided by the FLC, may be realized, and the equation that follows can be used to describe the behavior of the whole system. As a result, can be determined according to Eq. (15).

$$CD(t) = D(t) - D(t-1). \tag{15}$$

Fuzzification

It is the transformation of actual values into linguistic value. Every fuzzy system has a subset rule. Here, the members of the variable are depicted as positive and negative with various membership functions. Calculation of the membership functions for each variable may then take place as a result of the fuzzy partition being determined. The membership function may be defined as following Eq. (16) (Anurag et al. 2016), taking into consideration the most frequent symmetric triangular type:

$$\mu\left(x_i\right) = 1 - \frac{\left|x - x_i\right|}{\varepsilon_{x_i}}. \tag{16}$$

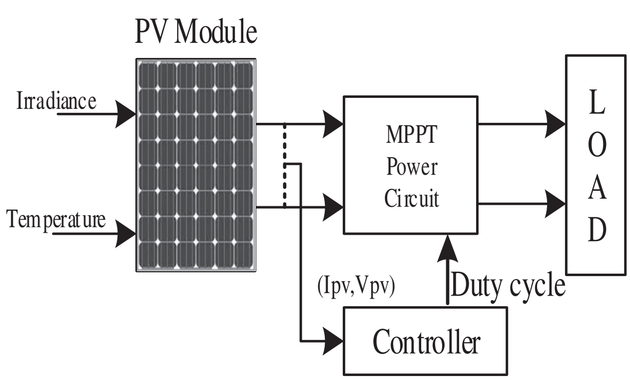

Fig. 4 MPPT control through input parameters

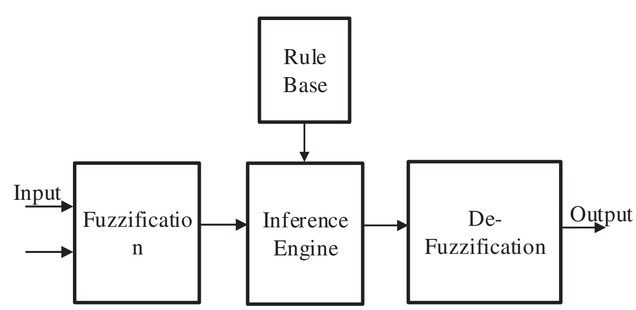

Fig. 5 Different stages in Fuzzy logic controller

Table 1 Rules of fuzzy logic controller

Fuzzy rule		Error E(n)				
		NB	NS	ZE	PS	PB
Change in error ΔE(n)	PB	ZE	ZE	PS	PS	PB
	PS	NS	ZE	ZE	PS	PS
	ZE	NS	ZE	ZE	ZE	PS
	NS	NS	ZE	ZE	ZE	PS
	NB	NB	NS	NS	ZE	ZE

NB negative big, *NS* negative small, *ZE* zero, *PS* positive small, *PB* positive big

Rule base

The inference engine creates new rules by applying logical rules to the rule base. The rule that was given to the MPPT block in the FLC design assigned several levels to the input variable as well as the output variable. These levels are as follows:- NB (negative big), NS (negative small), ZE (Zero), PB (Positive big), and PS (positive small). The sample sequence is given the variables, and those variables are given to it with regard to the sampling time. During the process of fuzzification, the numerical input is converted into a linguistic variable that is determined by the membership function. While designing the rules for MPPT, one must keep in mind the fact that any change in voltage will result in an increase in power. This must be kept in mind throughout the rule-making process. When there is an increase, the direction of the change continues to move in the same direction; but, when there is a decline, the direction of the change moves in the opposite direction (Gupta et al. 2016). After the theoretical designing of the membership function and the rules, which were then modified with the mistakes in order to reach the maximum performance (Figs. 6, 7, 8) .

Defuzzification

The transformation of an uncertain value into a precise value may be accomplished by taking the combination of the outputs from each rule. The primary objective of the defuzzification process is to convert the fuzzy set that was produced as a consequence of the aggregation into a numerical value that the designer can work with (specifically, the value of the tracking step ΔV). It is possible to use at least seven different defuzzification operators, but the one that is utilized the most is called the centroid, which is also known as the center of gravity. The Matlab fuzzy toolbox can calculate it for any input if all of the membership functions and If-then rules have been constructed. The whole range of output values, denoted by ΔV that corresponds to the variance in the values of inputs E and ΔE over the universe of discussion are shown in the Figure. The voltage and current of the SPV are represented in the flowchart by Vpv and Ipv. This optimizes the operating point of the PV by feeding the converter the SS reference voltage (Vpv). The input (E and △E) and output (△D) variables are fuzzified using

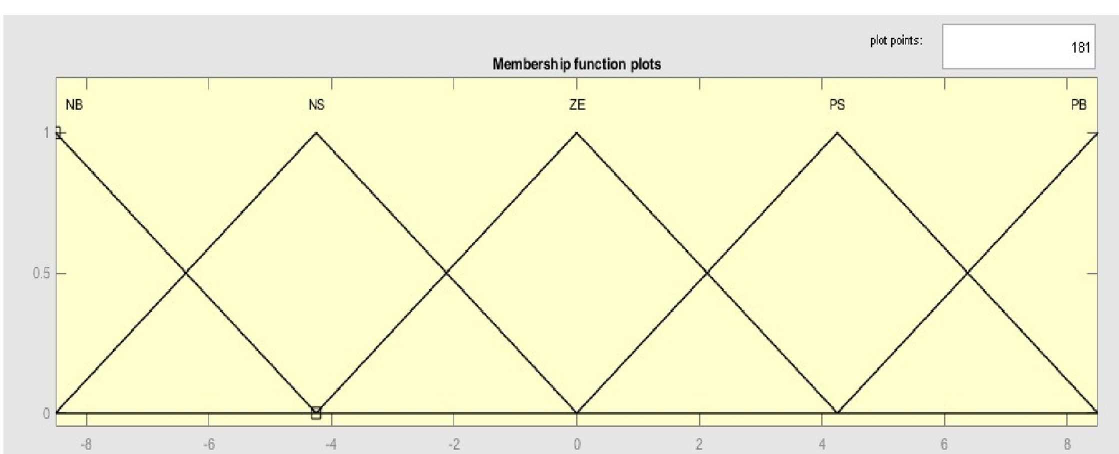

Fig. 6 Input membership function 1(mf1)

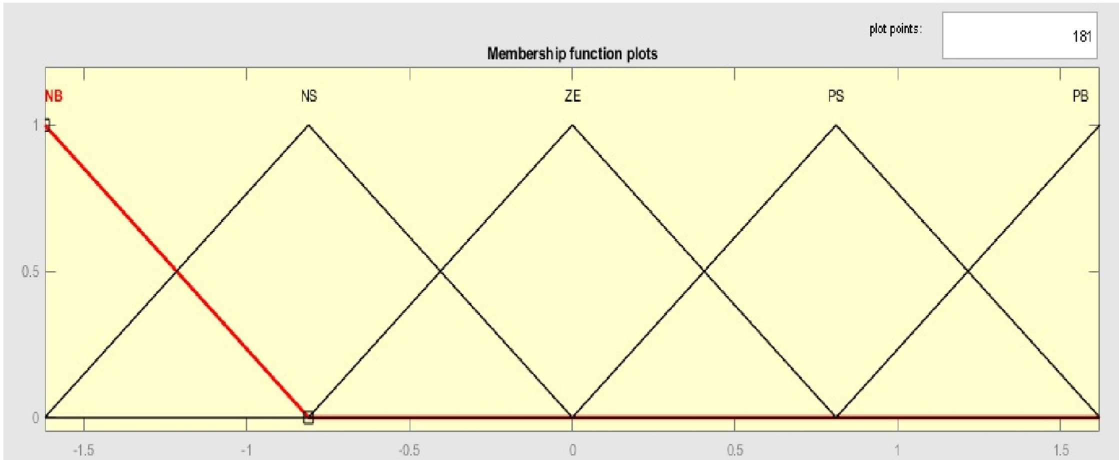

Fig. 7 Input membership function 2(mf2)

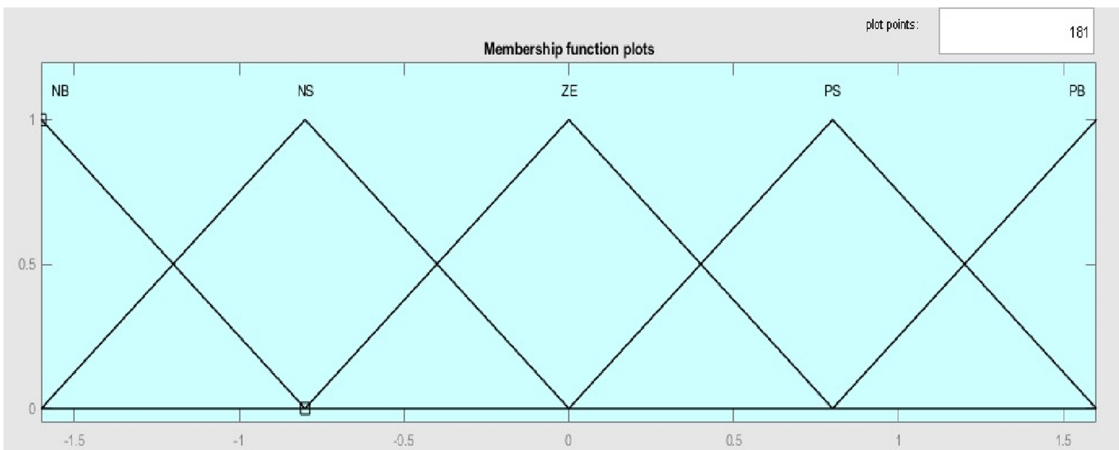

Fig. 8 Output membership Function

five different membership functions (MFs). These variables are related using the triangular MF. The controller, as shown in Table 1, contains 25 rules and is formatted in an "if" and "then" manner. The inference block in a fuzzy system can be shown as a surface plot, as in Fig. 9, and it maps the input variables with the output variables. Using Mamdani's technique, fuzzy rules are created. For all the input and output variables, five fuzzy levels are employed (see Fig. 10).

The Table 1 displays the proposed rules. The solar system's maximum power point will be tracked by the fuzzy rules as the severe weather conditions. When developing these rules, the rapidly varying solar radiation is taken into account. Here, triangular membership functions (mf) were

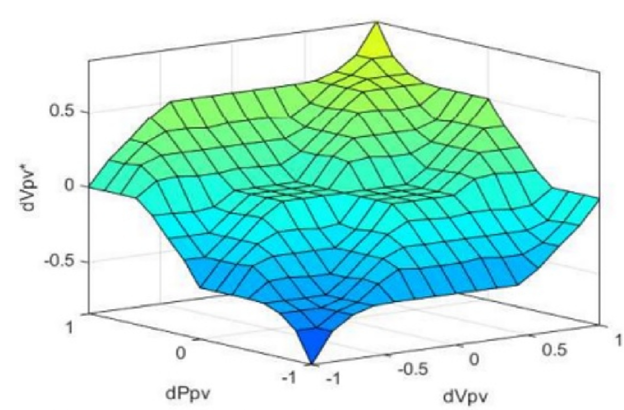

Fig. 9 Surface plot for fuzzy logic rules

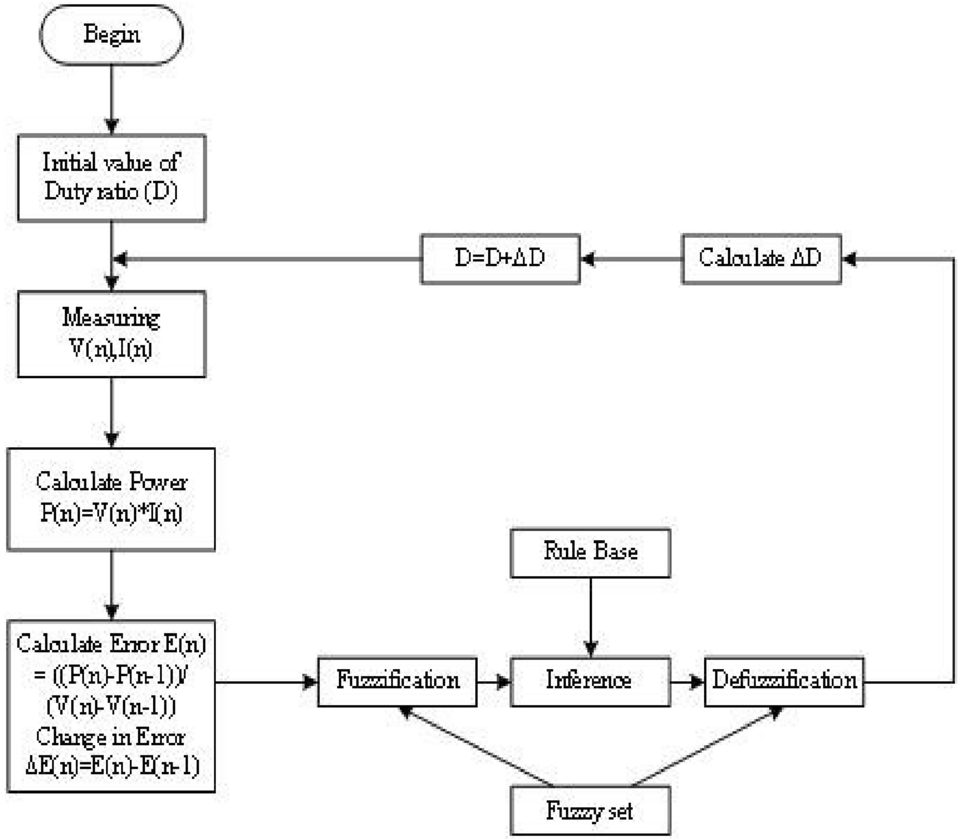

Fig. 10 Flow chart of fuzzy logic

employed. The range for the membership function is chosen by examining the oscillation of every signal.

The rules in the preceding table are construed as follows:

1 If (Change in Error is PB) and (Error is NB) then (Change in Duty Cycle is ZE).
2 If (Change in Error is PB) and (Error is NS) then (Change in Duty Cycle is ZE).
3 If (Change in Error is PB) and (Error is ZE) then (Change in Duty Cycle is PS).
4 If (Change in Error is PB) and (Error is PS) then (Change in Duty Cycle is PS).
5 If (Change in Error is PB) and (Error is PB) then (Change in Duty Cycle is PB).
6 If (Change in Error is PS) and (Error is NB) then (Change in Duty Cycle is NS).
7 If (Change in Error is PS) and (Error is NS) then (Change in Duty Cycle is ZE).
8 If (Change in Error is PS) and (Error is ZE) then (Change in Duty Cycle is ZE).
9 If (Change in Error is PS) and (Error is PS) then (Change in Duty Cycle is PS).
10 If (Change in Error is PS) and (Error is PB) then (Change in Duty Cycle is PS).
11 If (Change in Error is ZE) and (Error is NB) then (Change in Duty Cycle is NS).
12 If (Change in Error is ZE) and (Error is NS) then (Change in Duty Cycle is ZE).
13 If (Change in Error is ZE) and (Error is ZE) then (Change in Duty Cycle is ZE).
14 If (Change in Error is ZE) and (Error is PS) then (Change in Duty Cycle is ZE).
15 If (Change in Error is ZE) and (Error is PB) then (Change in Duty Cycle is PS).
16 If (Change in Error is NS) and (Error is NB) then (Change in Duty Cycle is NS).
17 If (Change in Error is NS) and (Error is NS) then (Change in Duty Cycle is NS).
18 If (Change in Error is NS) and (Error is ZE) then (Change in Duty Cycle is ZE).
19 If (Change in Error is NS) and (Error is PS) then (Change in Duty Cycle is ZE).
20 If (Change in Error is NS) and (Error is PB) then (Change in Duty Cycle is PS).
21 If (Change in Error is NB) and (Error is NB) then (Change in Duty Cycle is NB).
22 If (Change in Error is NB) and (Error is NS) then (Change in Duty Cycle is NS).
23 If (Change in Error is NB) and (Error is ZE) then (Change in Duty Cycle is NS).
24 If (Change in Error is NB) and (Error is PS) then (Change in Duty Cycle is ZE).

25 If (Change in Error is NB) and (Error is PB) then (Change in Duty Cycle is ZE).

The FLC's intended inputs are variations in the voltage of the solar photovoltaic panel (ΔV) and variations in the power of the solar photovoltaic panel (ΔP). The FLC's intended output is (ΔD), which is used by the PWM modulator to generate switching pulses.

Result and discussion

In the MATLAB/Simulink model, a photovoltaic (PV) system is constructed by taking into account the 1STH-215-P module parameters datasheet, which is shown in Table 2. The MATLAB/Simulink environment was used to simulate the proposed photovoltaic (PV) system with a Boost converter (BC), coupled with a maximum power point tracking (MPPT) device and a pulse width modulation (PWM) generator.

The Figs. 11 and 12 illustrates the P–V and I–V characteristics of a 1STH-215-P model 215 W PV system, and the Figure illustrates the P–V and I–V characteristics of a 215 W PV system that is created from a 1STH-215-P module by connecting one series module per string and one string in parallel.

To analyze the effectiveness of the developed PV system, various solar irradiation data profiles and ambient temperatures are taken into account in the vicinity of 25.1383°N, 75.8076°E in the month of 10 Feb 2023 to 25 Feb 2023, as shown in the Tables 2 and 3 respectively. The statistics show that the major factors for the production of electricity from a PV system, irradiance, and temperature, are non-linear throughout the day and year. The greatest temperatures and irradiance may be attained between 10:00 and 3:00 PM.

To analyze the efficiency of the proposed PV system, various solar irradiation data profiles along with ambient temperatures are taken into account in the nearby area of 25.1383°N, 75.8076°E in the period of 10 Feb 2023 to 25 Feb 2023, as shown in Tables 3 and 4 respectively. The statistics show that the major factors for the generation of power from a PV system, irradiance, and temperature, are non-linear throughout the day and year. The greatest temperatures and irradiance may be attained between 10:00 AM and to 3:00 PM. And because of the high temperature and irradiation levels on 25 Feb, electricity output is greater than it is earlier days.

Table 2 Solar (PV) array rating and parameters

Parameter	Value
Model type	1 STH-215-P
No. of cell per module (N_{cell})	60
V_{oc} (V)	36.3
I_{sc} (A)	7.84
V_{mp} (V)	29.0
I_{mp} (A)	7.35
Strings connected in parallel	1
Modules connected in series per strings	1
Series Resistance (R_s)	0.3938
Parallel Resistance (R_{sh})	313.399

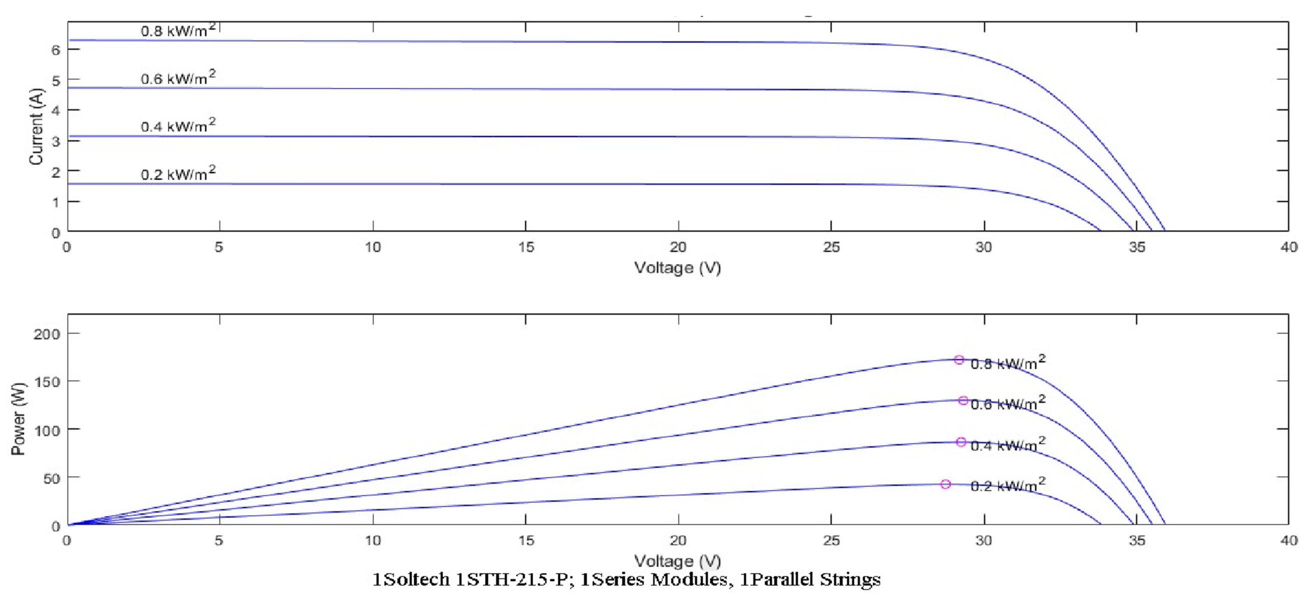

Fig. 11 Solar plate P–V and I–V characteristics for (800 W/m^2, 25 °C)

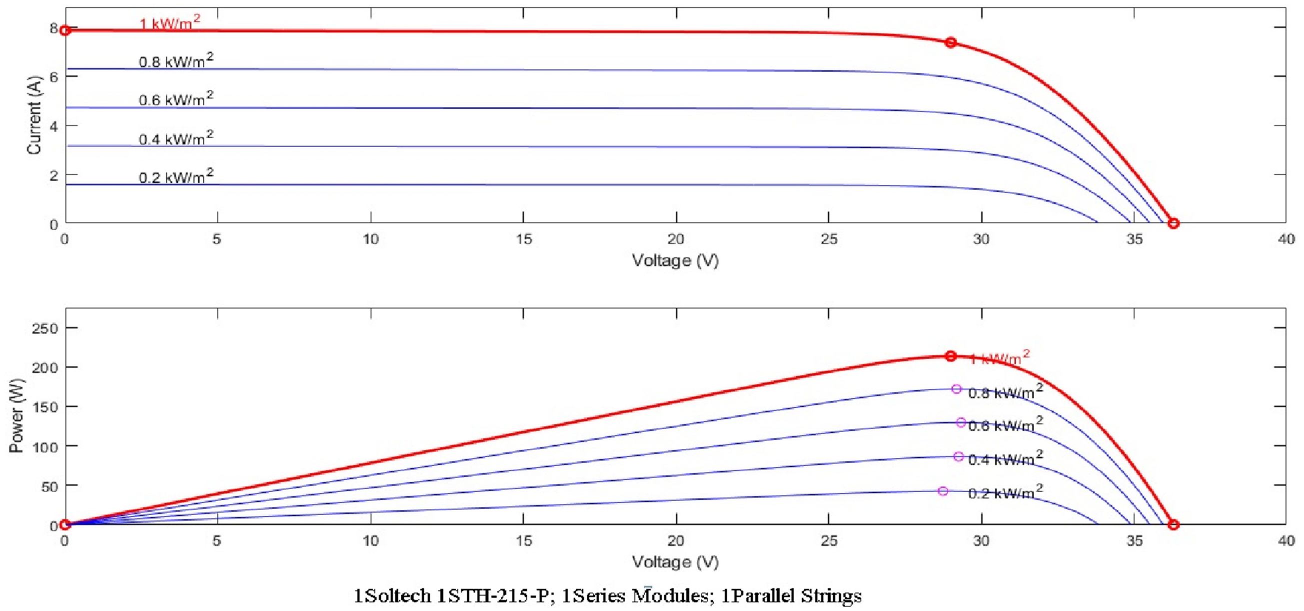

Fig. 12 Solar plate P–V and I–V characteristics for (1000 W/m^2, 25 °C)

Table 3 Availability of solar irradiance on 10 Feb 2023 to 25 Feb 2023

Irradiance (W/m^2)											
Time date	7:00	8:00	9:00	10:00	11:00	12:00	13:00	14:00	15:00	16:00	17:00
10-Feb-23	47	260	446	593	690	730	712	636	507	335	130
11-Feb-23	49	263	449	596	693	734	716	640	511	338	133
12-Feb-23	52	265	452	599	697	738	719	643	514	341	136
13-Feb-23	54	268	456	603	700	741	723	646	517	344	139
14-Feb-23	57	271	459	606	704	745	726	650	521	347	141
15-Feb-23	60	275	462	610	707	748	730	653	524	350	144
16-Feb-23	63	278	466	613	711	752	734	657	527	353	147
17-Feb-23	66	281	469	617	715	756	737	660	530	356	149
18-Feb-23	69	284	472	621	718	759	741	664	533	359	152
19-Feb-23	72	287	476	624	722	763	744	667	537	362	154
20-Feb-23	75	291	480	625	630	739	674	658	540	365	157
21-Feb-23	78	291	483	631	730	770	751	674	543	367	160
22-Feb-23	81	298	485	635	733	575	755	495	528	349	156
23-Feb-23	62	231	364	635	713	778	572	632	476	373	164
24-Feb-23	64	219	373	499	591	624	575	531	487	341	152
25-Feb-23	91	308	498	647	745	785	765	591	490	378	169

Figures 13, 14, 15, 16, 17 shows the result of power output by applying fuzzy logic controller with respect to without fuzzy logic controller as we seen the power fluctuation will be reduce by applying fuzzy logic controller. The output data reveals that as the solar irradiation falling on the solar panels is distorted by the environment's clouded sky, the output power of the PV system greatly depends on the solar irradiation and temperature data. The output power that is acquired fluctuates from time to time, but on average, the peak power is attained between 10:00 and 15:00. According to data from 22, 23, 24 Feb 2023, the system saw a dramatic dip and surge in power generation, which is caused by the presence of clouds in the targeted areas. There are minor changes in the values of temperature and irradiances from 10 to 25 Feb.

The maximum output voltage, current, and power obtained from the PV panel at each respective time will be shown in the given Table 5.

Table 4 Temperature on 10Feb 2023 to 25 Feb 2023

Temperature (°C)											
Time date	7:00	8:00	9:00	10:00	11:00	12:00	13:00	14:00	15:00	16:00	17:00
10-Feb-23	16	19	23	26	29	30	31	32	32	32	30
11-Feb-23	16	19	22	25	27	29	30	30	30	30	28
12-Feb-23	14	16	20	23	25	26	28	28	28	27	26
13-Feb-23	11	13	16	19	22	24	25	26	26	26	25
14-Feb-23	12	17	20	23	26	27	28	29	30	29	28
15-Feb-23	13	18	22	26	28	30	31	32	33	32	30
16-Feb-23	15	19	23	26	28	30	32	33	33	32	30
17-Feb-23	15	18	22	24	27	29	31	32	32	31	30
18-Feb-23	15	18	23	26	28	30	31	32	32	32	30
19-Feb-23	15	19	23	27	30	31	32	33	33	33	32
20-Feb-23	18	21	25	28	31	33	34	34	35	34	32
21-Feb-23	18	21	25	28	31	32	33	34	34	34	32
22-Feb-23	18	21	23	26	29	30	31	32	32	32	31
23-Feb-23	19	20	23	26	28	30	31	32	32	32	30
24-Feb-23	18	20	23	26	29	30	31	32	32	32	31
25-Feb-23	18	21	24	27	30	32	33	33	33	33	31

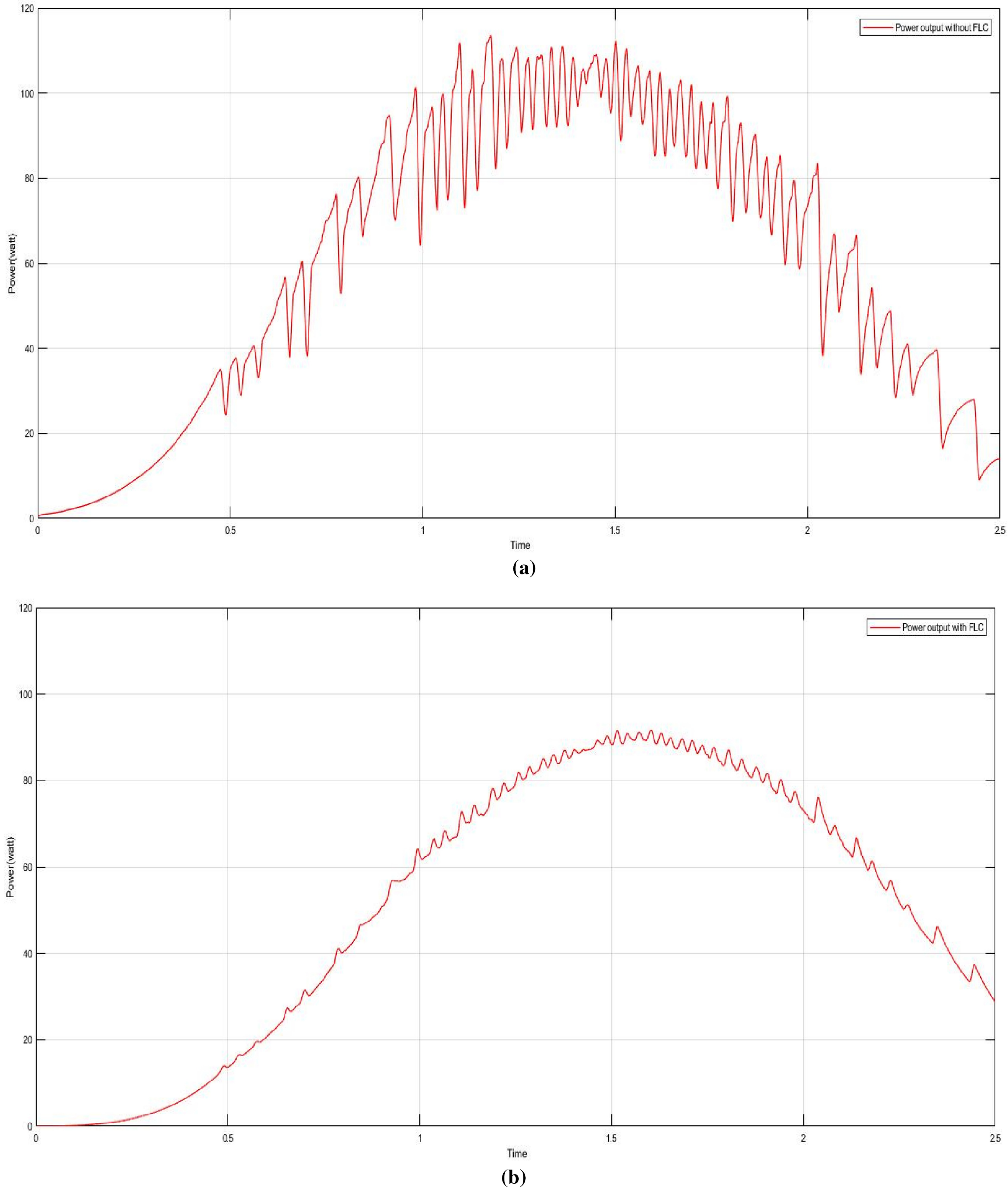

Fig. 13 **a** Power output without fuzzy logic controller at 21 Feb. **b** Power output with fuzzy logic controller at 21 Feb

The output voltage on February 20, 22, 23, and 24 was abruptly reduced owing to overcast and cold weather conditions that were present during that period. However, the low amount of voltage that was generated on February

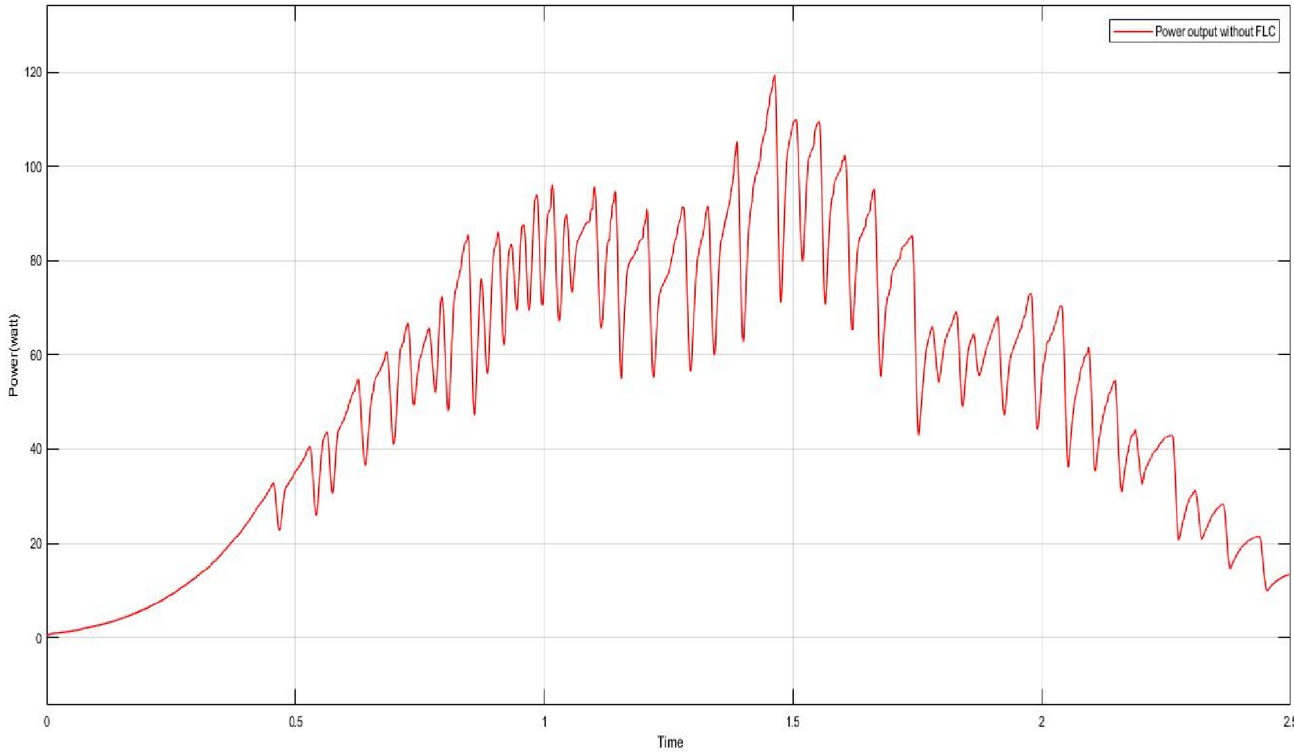

(a)

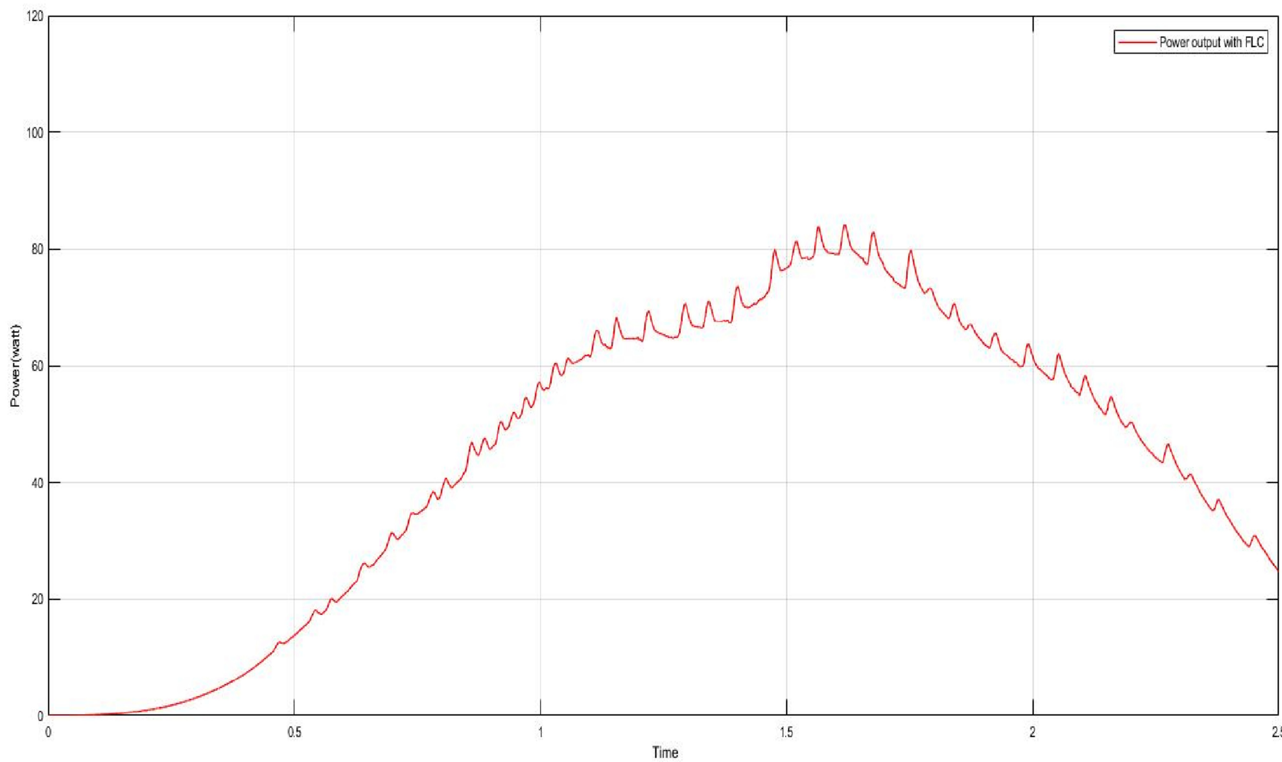

(b)

Fig. 14 **a** Power output without fuzzy logic controller at 22 Feb. **b** Power output with fuzzy logic controller at 22 Feb

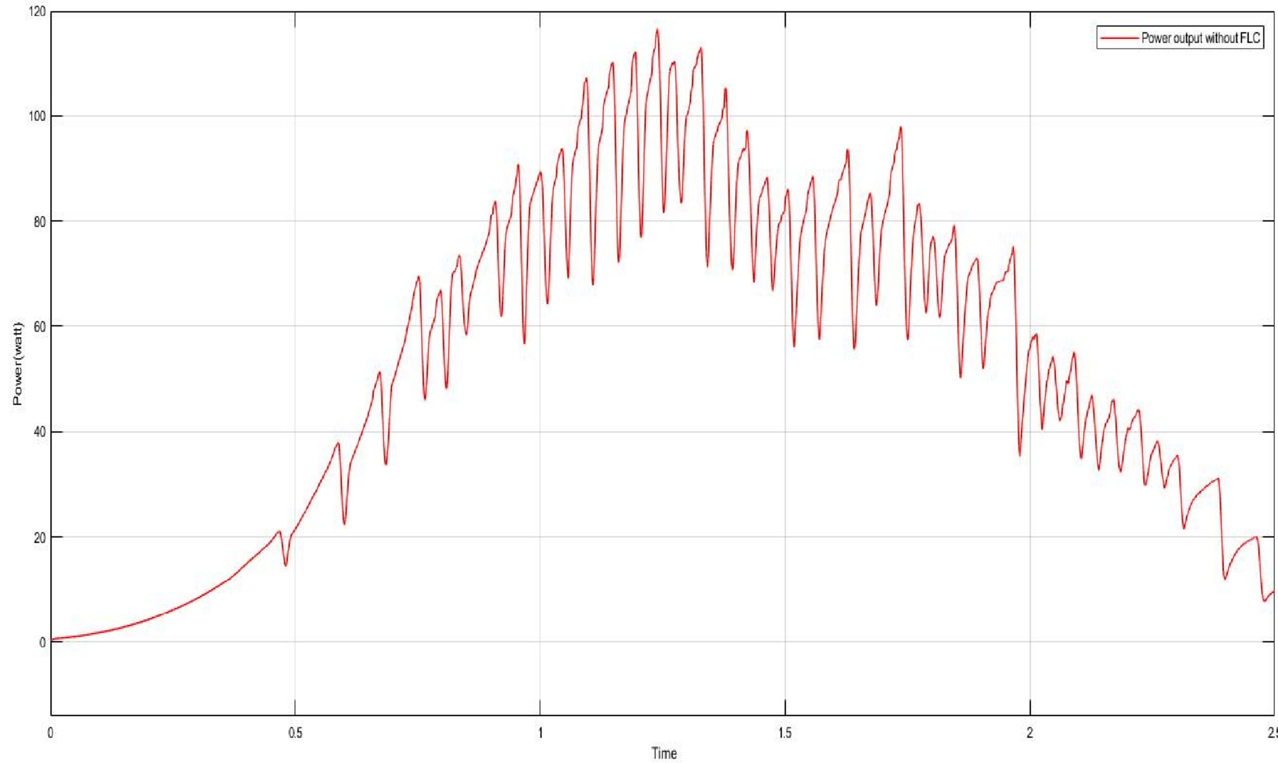

(a)

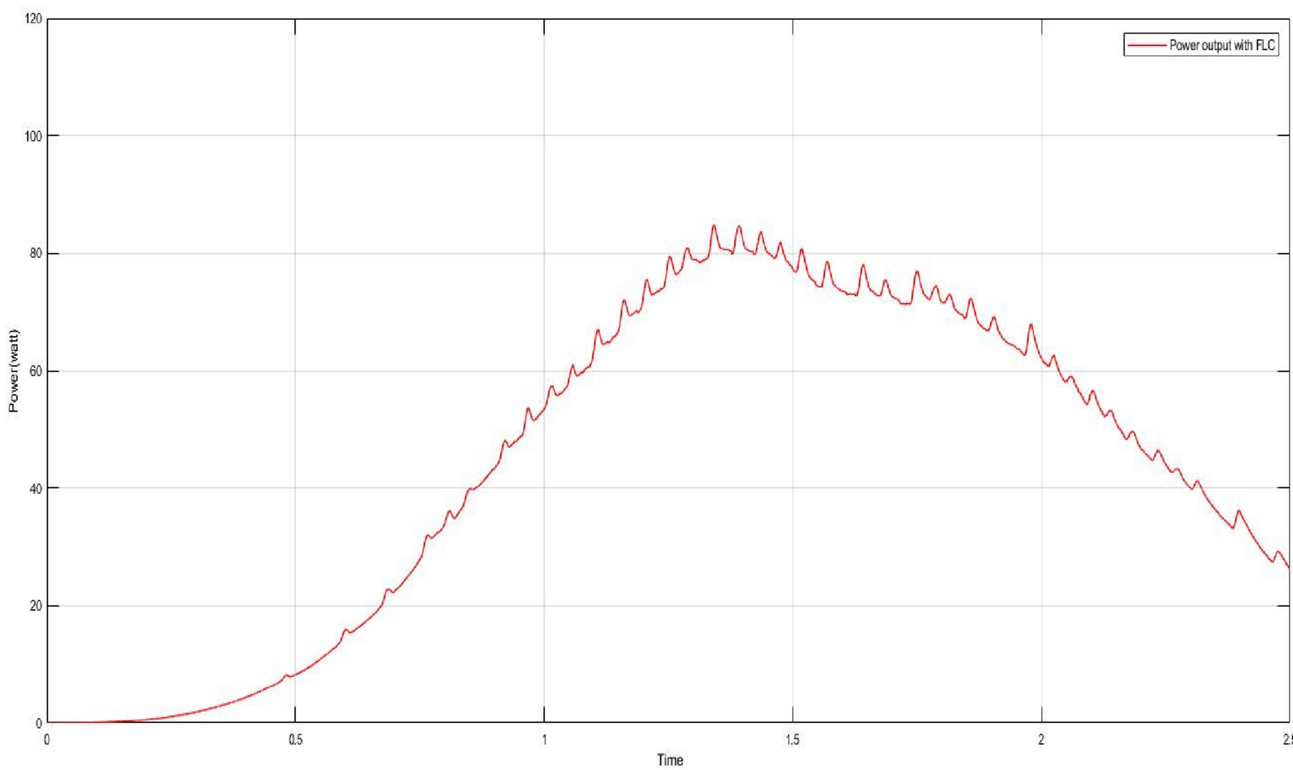

(b)

Fig. 15 **a** Power output without fuzzy logic controller at 23 Feb. **b** Power output with fuzzy logic controller at 23 Feb

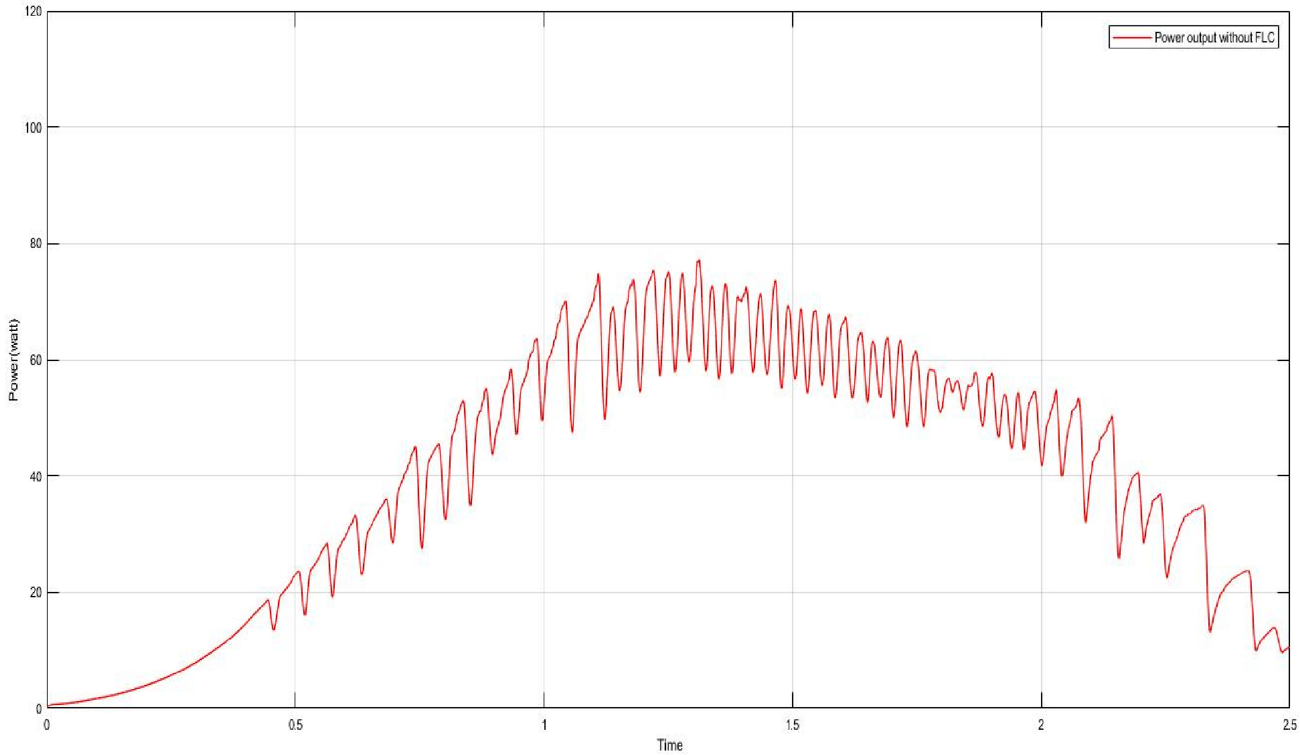

(a)

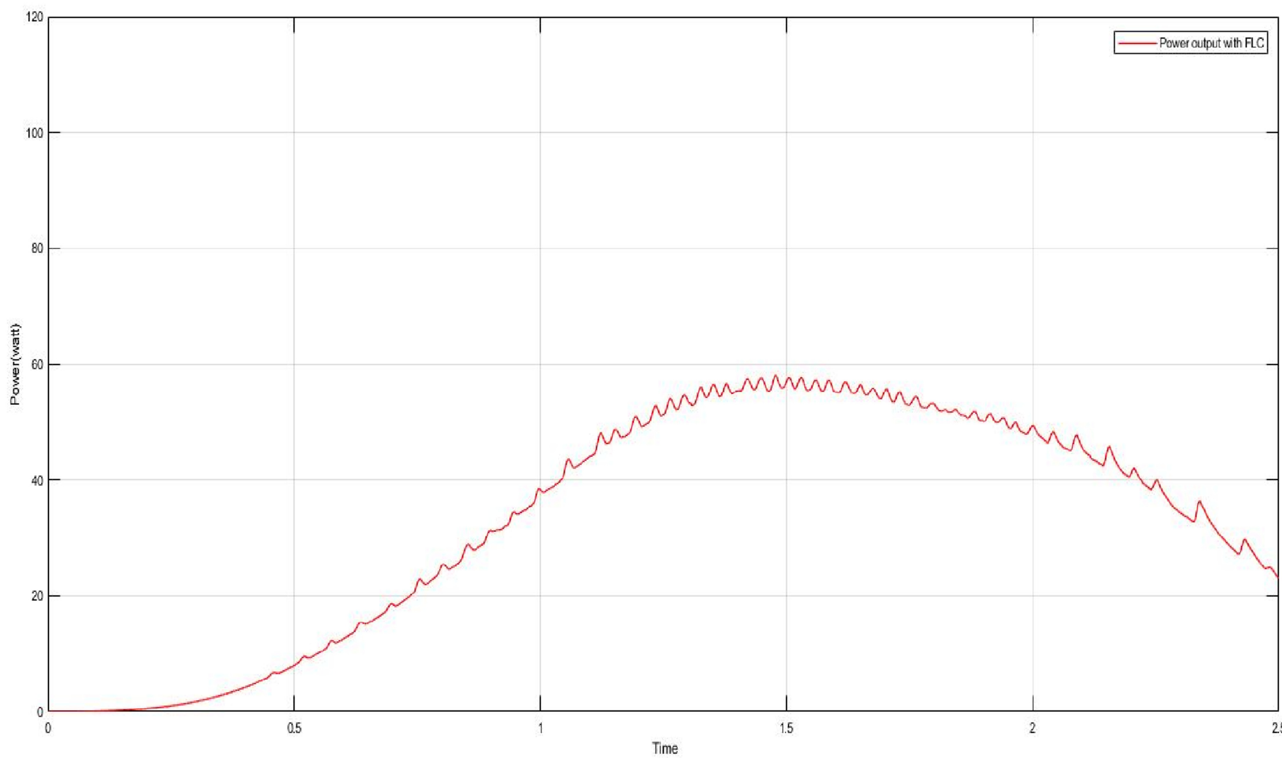

(b)

Fig. 16 **a** Power output without fuzzy logic controller at 24 Feb. **b** Power output with fuzzy logic controller at 24 Feb

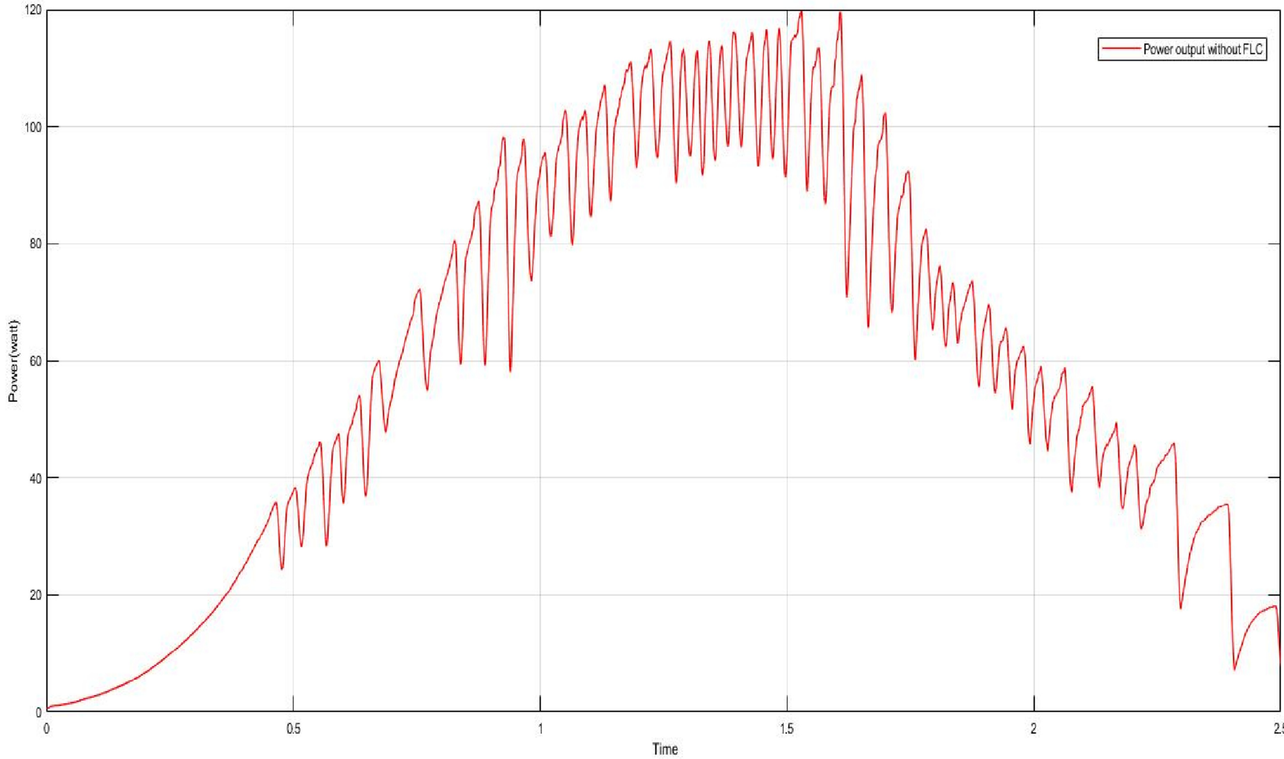

(a)

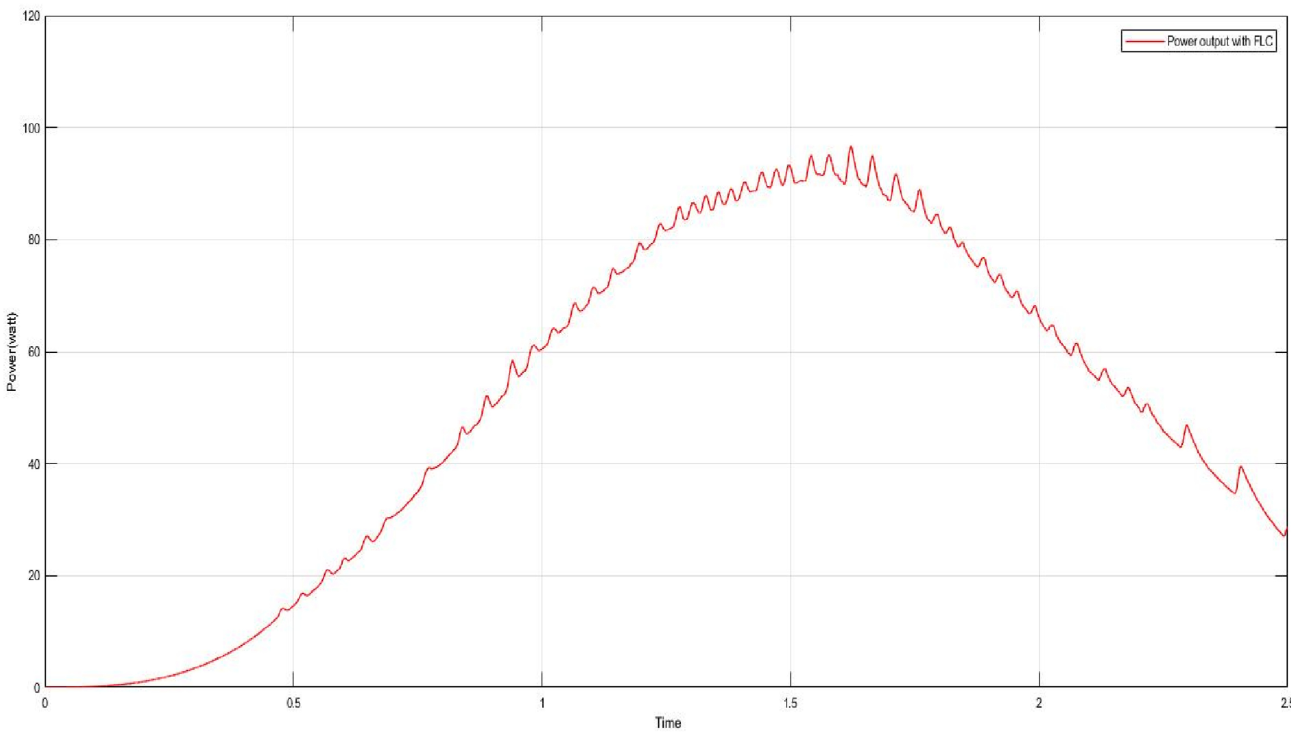

(b)

Fig. 17 **a** Power output without fuzzy logic controller at 25 Feb. **b** Power Output with fuzzy logic controller at 25 Feb

Table 5 Output voltage, current and power on 10 Feb 2023 to 25 Feb 2023

Date	Output voltage	Output current	Output power
10-Feb-23	45.01	1.80	81.03
11-Feb-23	45.47	1.819	82.7
12-Feb-23	45.32	1.813	82.14
13-Feb-23	45.52	1.821	82.89
14-Feb-23	45.68	1.827	83.48
15-Feb-23	46.64	1.866	87.01
16-Feb-23	46.86	1.874	87.84
17-Feb-23	46.82	1.873	87.67
18-Feb-23	46.87	1.875	87.86
19-Feb-23	47.35	1.894	89.66
20-Feb-23	44.72	1.789	79.79
21-Feb-23	47.86	1.915	91.64
22-Feb-23	45.87	1.835	84.16
23-Feb-23	46.04	1.842	84.80
24-Feb-23	37.72	1.509	56.91
25-Feb-23	48.97	1.959	95.93

24, 2023, was mostly due to the day's very gloomy weather conditions, which were the consequence of getting a very low value of solar irradiance and temperature. This was the primary cause of the low amount of voltage that was generated. These findings will be shown in this Fig. 18.

The output current on February 20, 22, 23, and 24 was abruptly reduced owing to overcast and cold weather conditions that were present during that period. However, the low amount of current that was generated on February 24, 2023, was mostly due to the day's very gloomy weather conditions, which were the consequence of getting a very low value of solar irradiance and temperature. This was the primary cause of the low amount of current that was generated. These findings will be shown in this Fig. 19.

The output power on February 20, 22, 23, and 24 was abruptly reduced owing to overcast and cold weather conditions that were present during that period. However, the low amount of power that was generated on February 24, 2023, was mostly due to the day's very gloomy weather conditions, which were the consequence of getting a very low value of

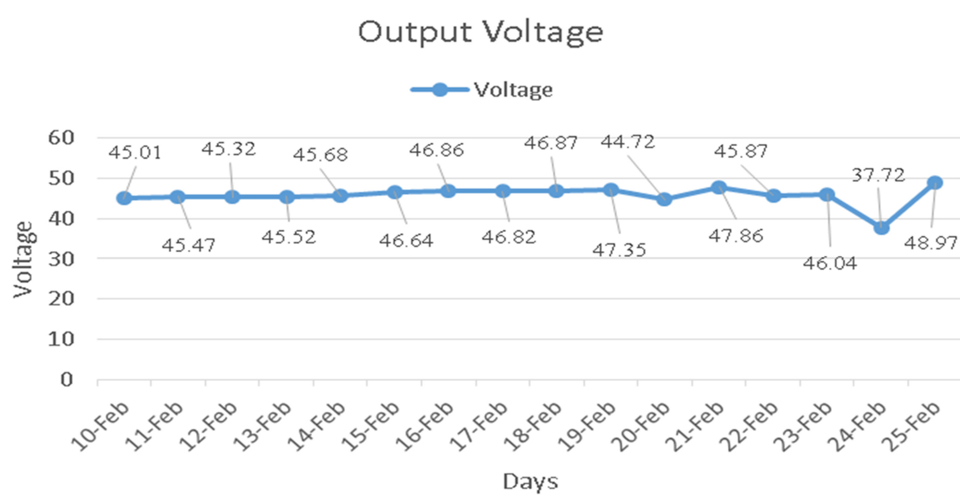

Fig. 18 Output voltage of 10 Feb 2023 to 25 Feb 2023

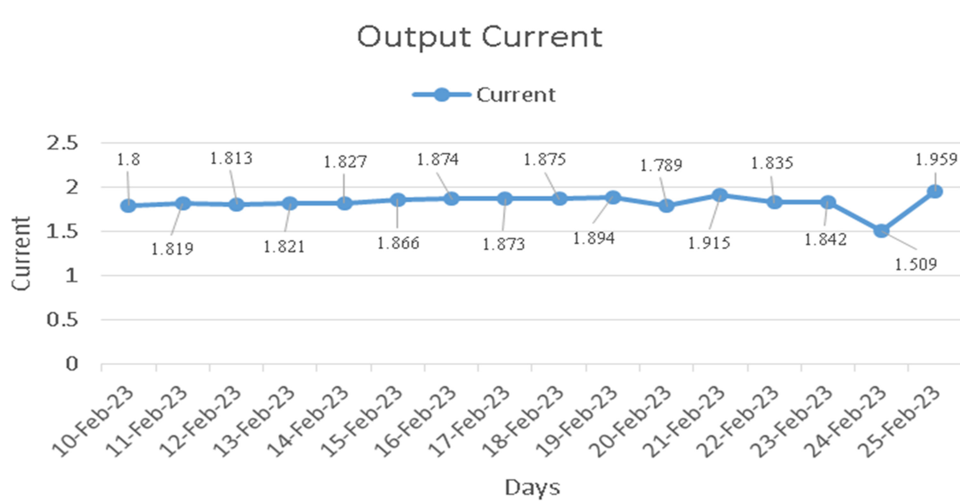

Fig. 19 Output current of 10 Feb 2023 to 25 Feb 2023

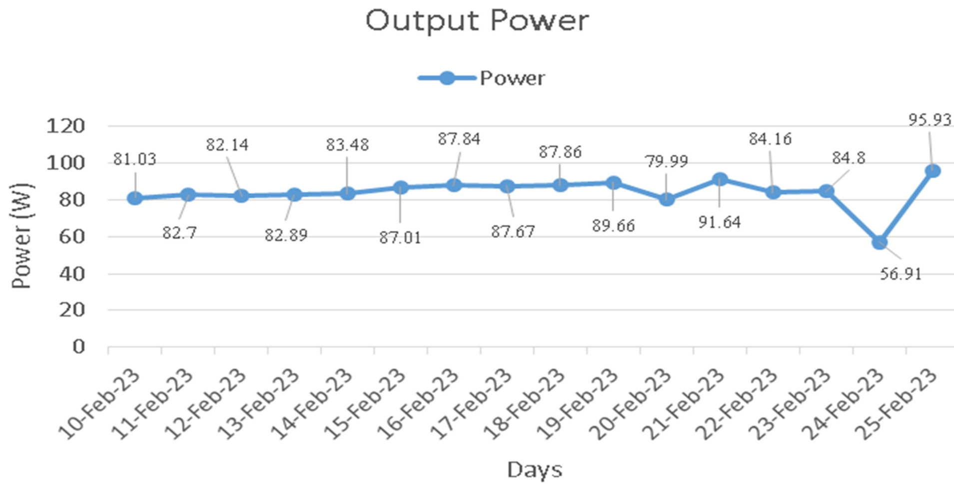

Fig. 20 Output Power of 10 Feb 2023 to 25 Feb 2023

solar irradiance and temperature. This was the primary cause of the low amount of power that was generated. These findings will be shown in this Fig. 20.

Conclusion

In this paper, a photovoltaic (PV) system that also includes a boost converter (BC) is constructed using the MATLAB/Simulink environment. An MPPT-based fuzzy logic controller is used in this study to match the reference output of the solar panel, which paves the way for a novel approach to the extraction of MPPs in situations that are prone to change. Subsequently, an FLC is combined with a step-up voltage converter to keep the waveform of the output voltage constant with the reference voltage input. The study results showed that the newly developed approach could accurately determine the maximum operated points in a shorter amount of time regardless of the rapid irradiance variations. The output power that is acquired fluctuates from time to time, but on average, the peak power is attained between 10:00 and 15:00. The input weather conditions are obtained from the area of 25.1383°N, 75.8076°E from 10 to 25 Feb 2023. This is done so that the constructed PV system may be analyzed using real-time data. The approach that was suggested has superior stability as well as high voltage gain while simultaneously reducing the amount of voltage stress experienced across the switch. According to the findings, the output power of the PV system is heavily dependent on the sun irradiation data, as well as the temperature data on the PV panels.

References

Anurag, A., Bal, S., Sourav, S., Nanda, M.: A review of maximum power-point tracking techniques for photovoltaic systems. Int. J. Sustain. Energy. **35**(5), 478–501 (2016). https://doi.org/10.1080/14786451.2014.918979

Eltamaly, A.M., Farh, H.M.H., Othman, M.F.: A novel evaluation index for the photovoltaic maximum power point tracker techniques. Sol. Energy **174**, 940–956 (2018). https://doi.org/10.1016/j.solener.2018.09.060

Gupta, A., Chauhan, Y.K., Pachauri, R.K.: A comparative investigation of maximum power point tracking methods for solar PV system. Sol. Energy. **136**, 236–253 (2016). https://doi.org/10.1016/j.solener.2016.07.001

Ibrahim, S.A., Nasr, A., Enany, M.A.: Maximum power point tracking using ANFIS for a reconfigurable PV-based battery charger under non-uniform operating conditions. IEEE Access **9**, 114457–114467 (2021). https://doi.org/10.1109/ACCESS.2021.3103039

Kumar, K., Babu, R.N., Prabhu, K.R.: Design and analysis of RBFN-based single MPPT controller for hybrid solar and wind energy system. IEEE Access **5**, 15308–15317 (2017). https://doi.org/10.1109/ACCESS.2017.2733555

Kumar, K., Prabhu, K.R., Ramesh Babu, N., Sanjeevikumar, P.: A novel six-switch power converter for single-phase wind energy system applications. Lect. Notes Electr. Eng. **435**, 267–275 (2018). https://doi.org/10.1007/978-981-10-4286-7_26

Pillai, D.S., Rajasekar, N., Ram, J.P., Kumar, V.: Design and testing of two phase array recon fi guration procedure for maximizing power in solar PV systems under partial shade conditions (PSC). Energy Convers. Manag. **178**, 92–110 (2018). https://doi.org/10.1016/j.enconman.2018.10.020

Saravanan, S., Babu, N.R.: Maximum power point tracking algorithms for photovoltaic system—a review. Renew. Sustain. Energy Rev. **57**, 192–204 (2016). https://doi.org/10.1016/j.rser.2015.12.105

Wang, H., Gaillard, A., Hissel, D.: A review of DC/DC converter-based electrochemical impedance spectroscopy for fuel cell electric vehicles. Renew. Energy. **141**, 124–138 (2019). https://doi.org/10.1016/j.renene.2019.03.130